Carbohydrate Polymers 95 (2013) 515–521

Contents lists available at SciVerse ScienceDirect

Carbohydrate Polymers

journal homepage: www.elsevier.com/locate/carbpol

Influence of water content and drying on the physical structure of native hyaluronan

Alena Průšová[a,b], Frank J. Vergeldt[a], Jiří Kučerík[b,*]

[a] Laboratory of Biophysics, Department of Agrotechnology & Food Sciences, Wageningen University, Dreijenlaan 3, 6703 HA, Wageningen, The Netherlands
[b] Institute of Environmental Sciences, University of Koblenz-Landau, Fortstrasse 7, 768 29 Landau, Germany

ARTICLE INFO

Article history:
Received 16 January 2013
Received in revised form 18 February 2013
Accepted 6 March 2013
Available online 16 March 2013

Keywords:
Hyaluronan
Hydration kinetics
Plasticization
Glass transition
DSC
TD-NMR

ABSTRACT

Hydration properties of semi-diluted hyaluronan were studied by means of time domain nuclear magnetic resonance. Based on the transverse proton relaxation times T_2, the plasticization of hyaluronan which was precipitated by isopropylalcohol and dried in the oven have been determined at water content 0.4 g of water per g of hyaluronan. Above this water content, the relaxation times increased and levelled off around 0.8 g of water per g of hyaluronan which agrees well with values determined earlier by differential scanning calorimetry and dielectric relaxometry. The freeze dried and oven dried samples showed differences in their physical structure such as glass transition, plasticization concentration and sample topography which influenced their kinetics and mechanisms of hydration. Results confirmed earlier hypothesis that some native biopolymer structures can be easily modified by manipulation of preparation conditions, e.g. drying, giving fractions with specific physicochemical properties without necessity of their chemical modification.

1. Introduction

Hydrated polysaccharides are nowadays the subject of intense research efforts motivated both by fundamental research and by their industrial applications, e.g. in cosmetics and pharmaceuticals. Hyaluronan (HYA) has received growing attention compared with other polysaccharides because of its biological activity, water-retention capacity and hydration properties (Garg & Hales, 2004). HYA is an anionic, unbranched, non-sulphated glycosaminoglycan composed of repeating disaccharides units (β-1-3 D-N-acetylglucosamine, β-1-4 D-glucuronic acid).

HYA is a main component of the extracellular matrix in connective, epithelial, and neural tissues (Garg & Hales, 2004) as well as the synovial fluid which lubricates and maintains the cartilage (Sutherland, 1998). HYA is a water-soluble polysaccharide that produces a viscoelastic fluid, but does not form a gel (Almond, DeAngelis, & Blundell, 2006). It is assumed that when dissolved in water, the antiparallel HYA chains overlap in a meshwork stabilized by specific H-bonds (i.e. up to five H-bonds per tetrasaccharide unit of HYA) and hydrophobic interactions. Such a highly cooperative structure is formally equivalent to the β-sheet formed by proteins (Scott & Heatley, 1999). Scott and Heatley conclude that the characteristic behaviour of HYA solutions is the molecular-mass-dependent transition between tertiary structures of β-sheet and 2-fold helices by which important biological properties are controlled (Scott & Heatley, 2002). HYA's polarity and the formation of such a meshwork is a potential reason for the higher osmotic pressure in solution which is the cause of HYA's high water retention capacity (Davies, Gormally, Wynjones, Wedlock, & Phillips, 1983).

HYA hydration is frequently studied by means of differential scanning calorimetry (DSC). The classical DSC approach, which includes cooling and thawing of water present in a biopolymer, has been used by many research groups (Hatakeyama & Hatakeyama, 2004; Liu & Cowman, 2000; Takahashi, Hatakeyama, & Hatakeyama, 2000). This approach allows the categorization of water into different fractions according to its behaviour during cooling. The water fraction, which is in intimate contact with HYA and does not freeze, is called "non-freezing water". Next water fraction which exhibits melting/crystallization, shows considerable supercooling, and significantly smaller enthalpy than the bulk water is referred to as "freezing-bound water". The third fraction is bulk water. The sum of the freezing-bound and non-freezing water fractions is the "bound water content". The concept of bound water in (bio)polymers has been questioned by some authors. Their alternative explanation is that such water is only restricted by the junction zones in gel-like structures (Belton, 1997), or as a consequence of further growth of ice crystals after transformation of the (bio)polymer from a rubbery state into a glassy one (Bouwstra, Salomonsdevries, & Vanmiltenburg, 1995). However, other authors have reported contrasting results which demonstrate that surface water shows a coherent hydrogen bond pattern with

* Corresponding author. Tel.: +49 (0)6341 280 31 582; fax: +49 (0)6341 280 31 576.
E-mail addresses: kucerik@uni-landau.de, kucerik@email.cz (J. Kučerík).

0144-8617/$ – see front matter © 2013 Elsevier Ltd. All rights reserved.
http://dx.doi.org/10.1016/j.carbpol.2013.03.031

a large, net dipole field (Yokomizo, Nakasako, Yamazaki, Shindo, & Higo, 2005). Such hydrogen bonds between water and biopolymers (proteins in this case) are stronger and have longer lifetimes compared with hydrogen bonds in bulk water (Chakraborty, Sinha, & Bandyopadhyay, 2007). That water is unavailable for colligative effects. Recently, an alternative approach based on water evaporation has been introduced. It was shown that in the course of water evaporation from a HYA solution a linear dependency of evaporation enthalpy normalized by dry mass was abruptly interrupted at $W_C = 0.34\ g_{H20}/g_{HYA}$. This revealed that at this particular water content the evaporation from HYA is compensated by another processes associated probably with heat release (Prusova, Smejkalova, Chytil, Velebny, & Kucerik, 2010). This value was confirmed when enthalpy of evaporation was determined at every conversion degree during water evaporation (Kucerik et al., 2011). In the comparative study by (Mlcoch & Kucerik, 2013) it was showed that in the concentration interval 0.1–2 $g_{water}/g_{polysaccharide}$ this abrupt process can be observed only in HYA. However, the hydration numbers determined by thermoanalytical techniques reflect the state of water under non-equilibrium conditions and in a particular temperature range.

Therefore the results obtained from DSC experiments should be verified using an independent technique such as for example nuclear magnetic resonance (NMR). Such a technique does not require extrapolation from observations made at temperatures far from the point of interest as is often done in the case of DSC. Besides, it is well known that the nuclear spin relaxation times, the spin-lattice relaxation time (T_1) and the spin–spin relaxation time (T_2) of hydrogen nuclei within water molecules are determined by the physicochemical environment of the water (Shapiro, 2011). Consequently, the measurement of proton nuclear spin relaxation times provides information on polymer–water interactions and water dynamics in such a system. In fact, water mobility slows because the water is involved in H-bonds and other weak interactions. Water mobility is also slower when it is restricted in pores or cavities formed by molecules for example water soluble HYA. Therefore proportionally shorter relaxation times are expected to be measured (Topgaard & Soderman, 2002).

Past efforts to develop techniques to reprocess polysaccharides have addressed mainly the hydrophobic/hydrophilic properties and gave little attention to how much the native structure was compromised or physically changed. Understanding how polysaccharides interact with themselves, each other, and with water in semi-diluted systems is of great importance as it determines its final structure and physical properties. As shown recently by Kucerik et al. (2011), HYA potentially has alternate physical structures due to the presence of two types of glycosidic bonds and variability of reactive groups. It has been suggested that manipulation of drying conditions could bring about differences in physical structure of HYA, thus extending the potential applications of native, chemically non-modified, HYA.

The first aim of this study is to test whether the results obtained by several DSC approaches under non-isothermal conditions reported recently (Prusova et al., 2010) are comparable with results obtained using time domain NMR (TD-NMR). It is shown that both approaches give comparable data and shed light on the processes taking part in HYA structure at low water content. It is shown that the above-mentioned compensating process is the plasticization point above which the HYA segments have higher molecular motion, i.e. the physical structure is more susceptible to any modification during drying. Therefore, the second aim of this study is to test whether using of various drying methods have an influence on the resulting physical structure (mechanical properties, pore sizes, and hydration kinetics) of native HYA. This was tested by means of DSC, TD-NMR, and Environmental scanning electron microscopy techniques.

2. Experimental

The sodium salt form of bacterial HYA with a molecular weight of 800 kDa (measured by size-exclusion chromatography, results not reported) was kindly provided by Contipro Pharma, Ltd. (Dolní Dobrouč, Czech Republic). This sample was prepared by precipitating the solution through the addition of isopropylalcohol and then oven-dried. This sample is referred to as precipitated hyaluronan (P-HYA) or as "original" HYA.

2.1. Sample preparation

Hyaluronan powder was put into standard 20 mm NMR tubes (two parallel samples were measured) which were then placed in a moisturizing container with 100% relative humidity at a constant temperature of 19 °C. Samples were regularly homogenized and measured every 48 h using TD-NMR. The increasing water content (W_C), i.e. mass of water per gram of hyaluronan, was determined by regularly weighing the HYA sample. In order to achieve a W_C of 1 or higher, liquid water was added and the sample was homogenized for a period of 72 h.

To study the effect of drying on the physical structure of HYA, the hyaluronan-water solution was prepared with a concentration of 2.5% (w/w) and stirred for 24 h at room temperature. Two different drying methods were used: static drying of the solution in an oven at 25 °C, and freeze-drying. Therefore, three different hyaluronan samples were obtained: (i) static dried in the oven (O-HYA), ii) freeze dried (F-HYA) and (iii) original HYA sample (P-HYA). The prepared samples were stored in the desiccator at 19 °C and studied using DSC and TD-NMR techniques.

2.2. Time domain NMR

Time domain nuclear magnetic resonance (TD-NMR) measurements were performed using a MiniSpec (Bruker, Germany) instrument, operating at the proton Larmor frequency of 7.5 MHz for protons. T_2 relaxation decays, as a function of the W_C of the sample, were obtained by applying the Carr–Purcell–Meiboom–Gill (CPMG) pulse sequence. Echo time was kept constant at 0.1 ms, and the number of echoes and repetitions was changed depending on the W_C. The repetition time between scans was five times T_1 to avoid the T_1 weighting. To calculate T_2 values, the transverse relaxation curves from CPMG decays were fitted with Eq. (1) using RI-WinFit software (Version 2.4, Resonance Instrument Ltd., Oxfordshire, United Kingdom) with either bi-exponential or tri-exponential functions (in dependency on statistical parameters such as χ^2, standard error and R^2):

$$F(t) = \Sigma A_i \exp\left(\frac{-t}{T_{2,i}}\right), \quad (1)$$

where A is amplitude, t is time and T_2 is spin–spin relaxation time. The experiments were carried out at 25 °C.

2.3. Environmental scanning electron microscopy (ESEM)

ESEM microscopy was carried out on a Quanta 250 instrument (FEI, Brno, Czech Republic) in a low vacuum mode. A large field detector (LFD) was used with voltage 2–10 kV and spot size 3–4. Depending on the sample structure, a pressure between 50 and 70 Pa was used. The dwell time for picture acquisition was 30 μs. All samples were stored and equilibrated in the desiccator over the NaOH pellets for 3 days prior to imaging.

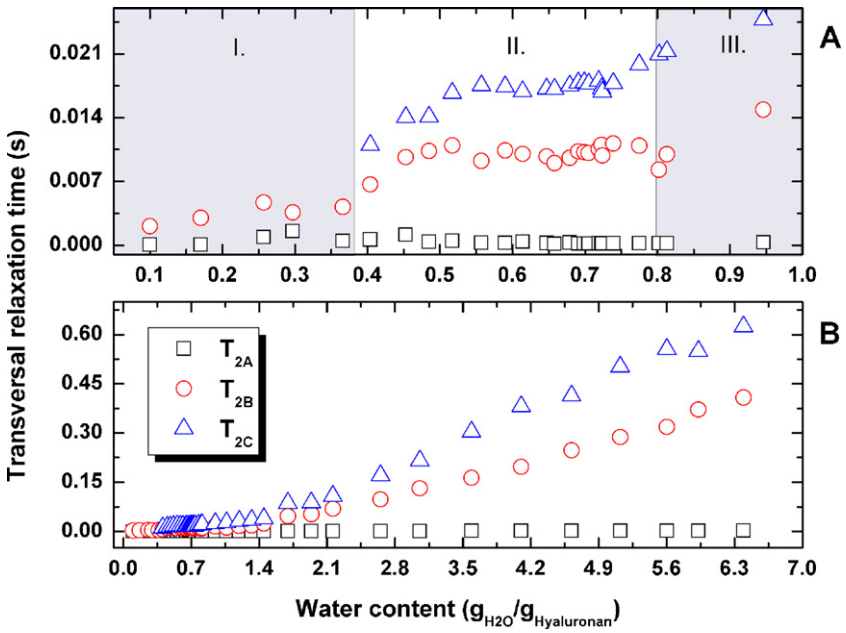

Fig. 1. T_2 relaxation times versus respective water fraction.

2.4. Thermal analysis

Differential scanning calorimetry (DSC) measurements were performed in order to analyze the difference in physical state of HYA samples obtained using various drying modes. The TA Instruments DSC Q1000, equipped with cooling accessory RCS90, was used and data were assessed by TA Universal Analysis 2000 software. The temperature and enthalpy calibration of the device were carried out using In and Sn as standards. Samples of approximately 5 mg (weighed to an accuracy of ± 0.01 mg) were placed in an aluminium open pan (Tzero® technology, DSC Q1000 TA Instruments). The following thermal protocol was used: started at 30.0 °C; equilibrated at −55 °C and then isotherm for 1 min. The next step was heating from −55.0 °C to 160 °C at four different heating rates: 30, 20, 10 and 5 °C min^{-1}. The flow rate of the dynamic nitrogen atmosphere was 50 mL min^{-1}.

It is necessary to point out that prior to data acquisition, samples were placed into the open DSC pan, cooled to −50 °C and then heated up to 150 °C before being cooled down again to −50 °C in order to set the same thermal history of the sample and evaporate the moisture from the HYA structure. This approach allowed the dependence of transitions on the heating rate to be tested.

The equilibrium moisture content of all three HYA samples and limits for DSC experiments, the temperature at which hyaluronan decomposition starts, were studied using evolved gas analysis, i.e. thermogravimetry (TG) coupled with mass spectrometry (MS) (NETZSCH STA 449 F3 Jupiter, Selb, Germany). Samples were placed into the alumina crucible and heated from room temperature to 800 °C at a rate of 5 °C min^{-1}. The reaction atmosphere was synthetic air, flow rate 50 mL min^{-1}.

3. Results and discussion

3.1. Hydration numbers determined with TD-NMR

Fig. 1 shows the transverse relaxation times determined by fitting Equation 1 to the transverse relaxation decay curves (not shown). As can be seen in Fig. 1A, for the low water content system (region I in Fig. 1A), two proton transverse relaxation times were determined: a slower one, T_{2B}, with an initial value of 2 ms, and a faster one, T_{2A}, with an initial value of 0.7 ms. Increasing the water content of the sample caused a moderate increase in T_{2A} and a more pronounced increase of T_{2B}. Upon reaching a W_C of around 0.4 g_{H20}/g_{HYA} (start of region II in Fig. 1A), a new proton pool with transverse relaxation time T_{2C} appeared. Both T_{2B} and T_{2C} irregularly but significantly grew with increasing water content. In contrast, the fastest component T_{2A} changed gradually to only 2.1 ms for the maximum water fraction investigated in this study i.e. $W_C = 6.5$ g_{H20}/g_{HYA} (Fig. 1B). Neither the standard deviation of the fitting nor the repeat measurements are shown in Fig. 1 as in all cases, the standard deviation is smaller than the symbol size and values of repetitive measurement are close to those reported in Fig. 1.

Multi-exponential behaviour of transverse relaxation decay curves, as observed in this study, is typical behaviour for viscoelastic systems like hydrated polysaccharides (Mariette, 2009). There are a number of mechanisms used as relaxation pathways in water–polysaccharide systems (McBrierty, Martin, & Karasz, 1999). Nevertheless proton exchange between polysaccharide hydroxyl protons and water molecules is thought to be the main relaxation mechanism in water–polysaccharide system (Okada, Matsukawa, & Watanabe, 2002) (Nestor, Kenne, & Sandstrom, 2010).

As can be seen in Fig. 1A, over the investigated water content range T_{2A} values are rather low. According to the Fuoss–Kirkwood distribution (Bakhmutov, 2004), such fast transverse relaxation can be attributed to transversal relaxation of large molecules, thus T_{2A} reflects relaxation of non-exchangeable HYA macromolecule protons. The slight increase in T_{2A} values over the range of W_C values is caused by gradual hydration of the hyaluronan structure which brings about an increase in hyaluronan macromolecule mobility.

As can be seen in Fig. 1A, a W_C of 0.4 g_{H20}/g_{HYA} is a border concentration above which a new proton pool T_{2C} is introduced. In general, water molecules are in mutual diffusive exchange. However, in the case of enormously rigid systems, when the water diffusion is sufficiently slow compared to the NMR time scale, relaxation is in the slow exchange regime and multi-component relaxation is observed. Consequently different water proton pools can be discriminated (Shapiro, 2011), i.e. T_{2B} and T_{2C} were observed. Above this border water content (0.4 g_{H20}/g_{HYA}) an abrupt increase in T_{2B} and T_{2C} values appears. This indicates changes in HYA structure

upon hydration. In a similar way, Froix & Nelson (1975) analyzed the state of water in cellulose and concluded that an abrupt increase of T_2 dependency on water content corresponds to the plasticization point above which both the cellulose chains and bound water acquire added modes of freedom (Froix & Nelson, 1975). This is in accordance with the behaviour of HYA in this study. In fact below this threshold the structure is "glass-like" and the gradual hydration brings about only a moderate increase in T_{2B} relaxation time. Conversely, above the plasticization concentration a significant increase in T_{2B} and T_{2C} can be observed (Fig. 1A) and the structure becomes "rubber-like". In other words, water molecules plasticize the structure and thus support molecular mobility, i.e. the structure is less rigid above this water content. As a result, water can much more easily penetrate the HYA structure. The value of this threshold ($W_C = 0.4\ g_{H20}/g_{HYA}$) agrees well with DSC results reported by Prusova et al. (2010) and Kucerik et al. (2011). In both cases it was concluded that during drying, when the water content corresponds to a value of around 0.34 g_{H20}/g_{HYA}, a competitive parallel process in HYA structure occurs. It was inferred that the formation of new intra/intermolecular interactions takes place which is associated with energy release. Thus, the results obtained in this study with TD-NMR indicate that this process is associated with a glass transition, which is known to be accompanied by the abrupt change in heat capacity (Wunderlich, 2005). In fact, the transition from a glassy into rubbery state increases the heat capacity of the system due to the higher mobility of chains and the free volume generated by segmental motion. Therefore, the compensation process detected by DSC during drying reported in (Prusova et al., 2010) is partially or fully caused by a decrease in heat capacity of the system.

The appearance of two components T_{2B} and T_{2C} reveals the existence of two types of water proton pools in HYA above the plasticization point. Since their transversal relaxation times are significantly lower than that of free water (around 2 s), it can be assumed that both proton fractions are affected by the presence of HYA macromolecules. The values of the relaxation times increased up to 0.5 and remained constant up to 0.8 g_{H20}/g_{HYA}. Above 0.8 g_{H20}/g_{HYA} (region III in Fig. 1A) a gradual increase in T_{2B} and T_{2C} values can again be seen. In fact, in the region from 0.5 to 0.8 g_{H20}/g_{HYA}, T_{2B} and T_{2C} values are rather short and close to T_{2A} values. It can therefore be concluded that this constant region can be seen as a saturation of the structure by water. With respect to recent results obtained using DSC (Prusova et al., 2010), we can assume that a water content of 0.5–0.8 g_{H20}/g_{HYA} is associated with the formation of non-freezing water fraction and some structural changes connected with wetting and swelling of HYA structure. Under experimental conditions, the driving force in water adsorption is the condensation of water vapor on curved surfaces and pores in accordance with the Kelvin and Young–Laplace equations. Moreover, adsorption onto polar groups of the HYA chain takes place and as a result, water bridges arise to stabilize the hydrated HYA structure leading the system to the lower energy (Almond et al., 2006; Nestor et al., 2010). DSC measurements on non-freezing water (Prusova et al., 2010) and dielectric relaxation (Hunger, Bernecker, Bakker, Bonn, & Richter, 2012) show the hydration number around 0.8 g_{H20}/g_{HYA}. It can therefore be assumed that both types of water, i.e. water proton pools with transversal relaxation times T_{2B} or T_{2C} below this W_C, represent the non-freezing water fraction.

The amplitudes of fitting (A), given by Eq. (1), are proportional to the relative fractions of protons involved in relaxation with T_2 longer than the echo time (the time between 90° and 180° radio frequency pulses) in CPMG pulse sequence. For $W_C = 0.75\ g_{H20}/g_{HYA}$, a ratio of amplitudes A_{2C}:A_{2B} is 5.8, which means that only 0.11 g of water per gram of HYA (ca. three water molecules per HYA disaccharide unit) have the faster relaxation time (T_{2B}) and thus these water molecules are more restricted in their motion. 0.64 grams of water per gram of HYA (fourteen water molecules per HYA disaccharide unit) is represented by T_{2C}. In light of the above discussion, a shorter T_{2B} relaxation time might notionally represent water integrated into HYA hydrophilic pores and therefore in intimate contact with polar groups. Due to free volume generation above the plasticization point, T_{2C} might represent water structurally restricted between hyaluronan chain double helices. This hypothesis is supported by the change in ratio between amplitudes upon increasing W_C: for $W_C = 2\ g_{H20}/g_{HYA}$ a ratio of amplitudes A_{2C}:A_{2B} is 0.6. This indicates that the progressive swelling, increase in pore size, and the collapse of present cavities causes a decrease in the proportional content of structurally restricted water. This was demonstrated by Kucerik et al. (2011) where for $W_C = 2\ g_{H20}/g_{HYA}$ the enthalpy of melting of ice formed in such cavities already resembled the melting enthalpy of pure water. This means the restriction of water is lower and hexagonal ice can be formed. It can be assumed that for sufficiently high values of W_C, components T_{2B} and T_{2C} will merge. It can be inferred from Fig. 1 that the dynamics of HYA hydration and/or drying are linked to complicated structural changes.

3.2. Morphology of the sample obtained under different drying conditions

3.2.1. Microscopy

Samples of HYA were prepared in three different ways as reported in the experimental section. First, the morphology of the surface was studied with electron microscopy under low vacuum conditions. Fig. 2A shows P-HYA. This sample shows a compact structure with heterogeneous surface features composed of both smaller and larger grains. It is also full of cavities and holes. This partially supports the statements from previous paragraph. Fig. 2B shows the hydrated surface of P-HYA (0.9 g_{H20}/g_{HYA}). The individual grains are swollen and mostly interconnected. On the other hand, F-HYA (Fig. 2C) shows a looser, crusty structure with a larger surface area. The surface is less heterogeneous than that of P-HYA. In Fig. 2D, we see O-HYA which shows a compact fragile structure with an even surface with no visible cavities or holes as in the case of P-HYA.

3.2.2. Phase transitions in the dried samples

The prepared HYA samples were tested by thermal analysis in order to observe differences in their physical structure. Prior to the DSC experiments, thermogravimetry coupled with mass spectrometry was used to determine the range of temperatures applicable for DSC and to determine the moisture content of the sample. Fig. 3 shows the mass loss and the ion current signals for CO_2 and H_2O as a function of temperature for the P-HYA sample. It can be seen that the temperature region up to 210 °C is associated only with the evaporation of moisture. Such a conclusion is based on the fact that up to 210 °C, there is only an ion current signal from H_2O and none from CO_2. Above 210 °C, a steep decrease in mass loss and the appearance of the first peaks in both the CO_2 and H_2O ion current signals indicates the beginning of HYA decomposition. Therefore DSC experiments can be performed up to a temperature of 200 °C.

The representative DSC record for different heating rates is depicted in Fig. 4. In the DSC record of all HYA samples, an exothermic peak occurs in the range −37 °C to −13 °C (marked as "I"). The peak temperature is heating rate dependent which indicates that this is a kinetic process. The exothermic peak "I" is followed by another two much smaller exothermic peaks. Thus, it is impossible to correctly determine the maxima of these two peaks. It is worth mentioning that the character of these peaks is independent of moisture content (tested in separate experiments – results not shown).

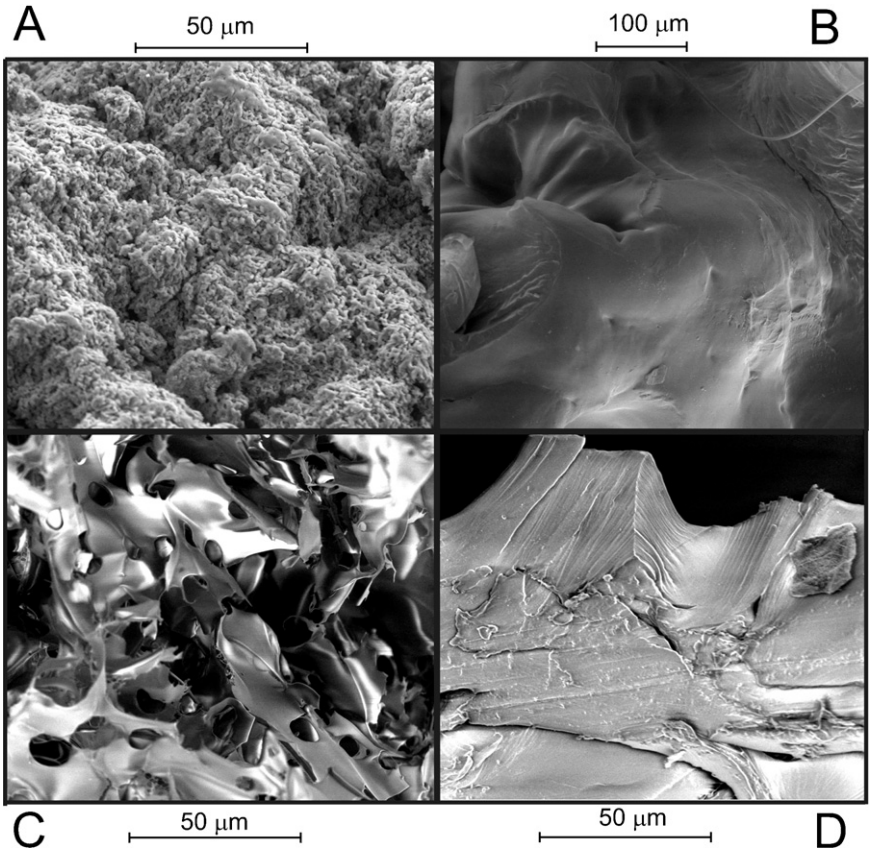

Fig. 2. ESEM image of different hyaluronan samples. (a) P-HYA, (b) F-HYA, (c) hydrated HYA ($W_C = 0.9\ g_{H20}/g_{HYA}$), (d) O-HYA.

Another thermal event appears in the 50–110 °C temperature range (marked as "II"). It is again dependent on the heating rate which implies that it is a kinetic process. In contrast to the exothermic peak "I" observed at low temperature, this thermal event "II" is dependent on the water content of the HYA sample, i.e. drying shifts this thermal event to higher temperature region.

The literature does not report much about the phase transitions in dry HYA. The dynamical mechanical analysis of the HYA film reported by Dave, Tamagno, Marsano, and Focher (1995) shows that the process occurring at room temperature is associated with the large-scale motion of the molecular chain segments, namely the glass transition. Observations of the kinetic character of process "II" in the present work are in line with this conclusion. Furthermore, the initial storage modulus E' of the HYA films decreased slightly as the temperature is raised from −100 °C up to −22 °C, and then showed simple discontinuity around 25 °C. Finally, it was shown an increase as the temperature was raised above 25 °C. This was considered a strain-induced crystallization with an increase in the

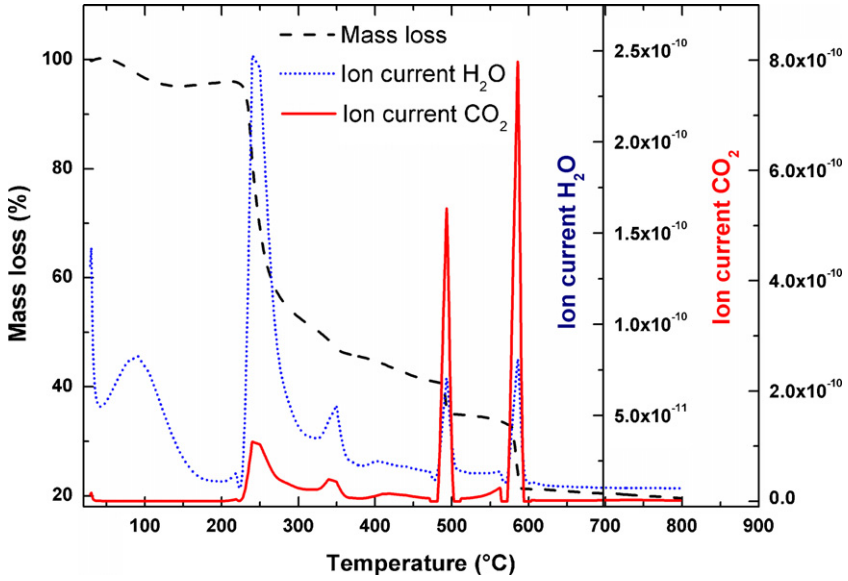

Fig. 3. TG and MS record of HYA, mass loss, CO_2 and H_2O ion current signals as a function of temperature.

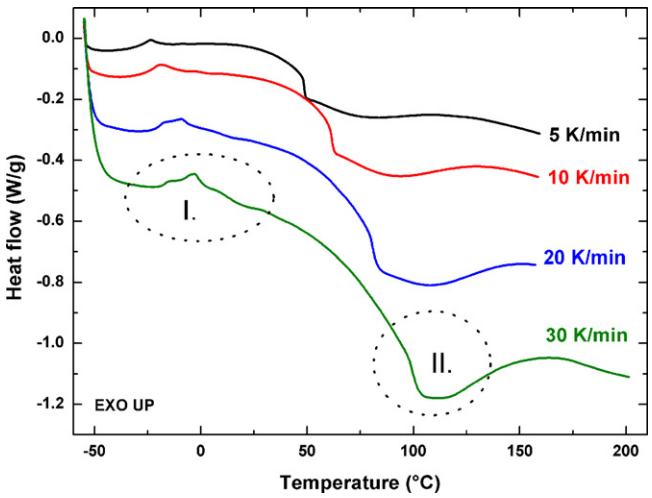

Fig. 4. The DSC record for the F-HYA sample (all runs were repeated twice).

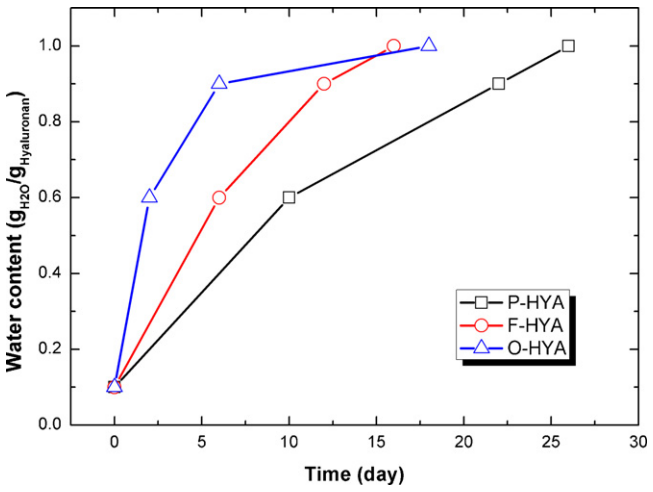

Fig. 5. Hydration progress for different HYA samples.

number of intermolecular and/or intramolecular hydrogen bonds before high-temperature relaxation phenomena occurred (Dave et al., 1995). Results shown in Fig. 4 support the hypothesis put forward by Dave et al. (1995) concerning the crystallization processes interrupted by glass transition. However, we can reject the hypothesis about its strain-induced origin since the process was observed using DSC in this work.

Table 1 summarizes the characteristic temperatures of both processes measured with DSC. The peak temperature in the crystallization process ("I") and the midpoint of the glass transition ("II") are both evaluated in the traditional way (Wunderlich, 2005). It can be seen that using different methods to dry the HYA has only a small effect on crystallization "I" but a pronounced effect on the amorphous transition "II". The temperature of the glass transition is highest for F-HYA and lowest for P-HYA. This means that from a mechanistic point of view, freeze-drying provides the most rigid structure at room temperature. The data in Table 1 shows the dependency of the glass transition temperature on the heating rate which allows extrapolation of glass transition temperature to quasi-isothermal conditions (the zero heating rate). The temperatures for quasi-isothermal conditions were for F-HYA = 34.7 °C, O-HYA = 28.7 °C, and P-HYA = 25.5 °C. This result indicates that at room temperature all samples are in the glassy state (below the glass transition temperature).

The temperature of the glass transition reflects the qualitative aspect of the amorphous phase while the change in the heat capacity associated with the glass transition provides more quantitative information. Put simply, the larger the change, the larger the part of the sample that is amorphous. Comparing changes in the heat capacities showed that the F-HYA sample exhibits the highest change in heat capacity (1.05 J g^{-1} K^{-1}) and O-HYA the lowest (0.1 J g^{-1} K^{-1}). The P-HYA sample showed a change in heat capacity of 0.7 J g^{-1} K^{-1}. We conclude that the O-HYA sample shows the lowest amorphous content. The recrystallization enthalpy calculation of exothermal peaks in area "I" gave for F-HAY = 3.21 J g^{-1}, P-HYA = 1.27 J g^{-1}, and O-HYA = 1.68 J g^{-1}. Those values reflect the energy necessary for reorganization of crystalline-like structures in individual HYA samples.

3.2.3. *Hydration characteristics of HYA samples prepared under different drying conditions*

In order to characterize the differences in the hydration characteristics of HYA samples, TD-NMR was used. All samples (P-HYA, O-HYA and F-HYA) were exposed to 100% relative humidity and analyzed as described in the experimental section. The plasticization point was determined in the same manner as in the Section 3.1, i.e. by the appearance of a new water proton pool. The results for the P-HYA sample were consistent with the previous results (Section 3.1); the plasticization point was determined as slightly below 0.4 g$_{H20}$/g$_{HYA}$. For the F-HYA sample, the plasticization point was between 0.55–0.65 g$_{H20}$/g$_{HYA}$ and for the O-HYA sample 0.8–0.9 g$_{H20}$/g$_{HYA}$. The plasticization order determined by TD-NMR is different from that determined by DSC, where the sample with the lowest plasticization temperature was P-HYA followed by O-HYA and finally the F-HYA sample (see Table 1). In fact, the plasticization points determined with TD-NMR and DSC differ in their physicochemical meaning. In TD-NMR, the plasticization point is a water content, and so is a measure of rigidity with water molecules acting as plasticizers. In the case of DSC experiments, the heat and associated temperature is the cause of higher molecular mobility and the glass transition. Those differences are clear indicators of the specificity of the HYA samples. It is worth mentioning that both techniques observe the same phenomenon i.e. glass transition, but under different conditions.

The TD-NMR data show the difference between the hydration mechanisms of the samples. As can be seen in Fig. 5, HYA samples have different kinetics of hydration, with O-HYA having the fastest. That can be explained by the lowest T_{2B} value (among three different HYA samples) up to W_C = 0.9 g$_{H20}$/g$_{HYA}$. Simultaneously, the associated amplitude, reflecting the proton fraction, is highest up

Table 1
The peak maxima and glass transition temperatures for different HYA samples.

HYA	Process "I" exothermic peak (°C)				Process "II" glass transition (°C)			
	Heating rate (°C/min)				Heating rate (°C/min)			
	30	20	10	5	30	20	10	5
P-HYA	−2.6	−8.8	−19.1	−24.4	81.5	65.3	45.9	36.2
O-HYA	−2.8	−8.6	−18.1	−23.9	87.7	72.7	52.8	41.5
F-HYA	−2.7	−9.2	−19.1	−23.7	99.2	82.7	61.6	48.6

to $W_C = 0.9\ g_{H20}/g_{HYA}$ and then is approximately equal to amplitude associated with T_{2C} relaxation time (data not shown). This means that below $0.9\ g_{H20}/g_{HYA}$, O-HYA has the largest fraction of structurally integrated water protons. In other words, O-HYA has the largest number of small pores. These cannot be seen from the scanning electron microscope pictures under applied conditions and resolution (Fig. 2), but explain the fast kinetics of hydration (see Fig. 5).

In our recent work, analysis of the P-HYA sample at different W_C values using DSC gave a plasticization point of $0.34\ g_{H20}/g_{HYA}$ (Prusova et al., 2010; Kucerik et al., 2011) which is in agreement with results obtained by TD-NMR in this work. In contrast, samples prepared under different drying conditions gave rather different results in terms of physicochemical properties and behaviour such as glass transition and response to the moisturizing conditions. This further emphasises our earlier statement that hydration, especially in the case of hyaluronan, is a "dynamic" value and reflects the sample's history (preparation, conditioning, drying...), the technique used for its determination, and slightly also the conditions under which the experiment is carried out.

4. Conclusion

In this study, HYA samples were prepared under three different drying conditions yielding the original, freeze-dried, and oven-dried HYA sample. It was demonstrated that DSC and TD-NMR are complementary techniques in terms of HYA hydration. The non-freezing water fraction in semi-diluted HYA can be determined using both techniques. Further, by using TD-NMR it is possible to determine the hydration kinetics of HYA and also to determine the water content of an HYA sample that corresponds to the glass-to-rubbery-state transition which is a measure of the rigidity of a system. The oven-dried sample has the fastest whereas the precipitated HYA sample has the slowest hydration kinetics. Based on the glass transition temperature, it was observed that the sample prepared by freeze-drying was the most rigid one and the oven-dried sample had the lowest amorphous fraction. Hence it was demonstrated that the supramolecular structure of native HYA is modified by drying conditions. This represents a promising strategy for further application of this polysaccharide in its native state, for example in the pharmaceutical industry in drug delivery systems with delayed wetting, swelling, and consequent release of transported drugs.

Acknowledgements

The authors wish to thank Prof. Dr. Gabriele E. Schaumann and Dr. Jette Schwarz from Universität Koblenz-Landau in Landau, Germany and Assoc. Prof. Dr. Henk Van As from Wageningen University, The Netherlands for their support and help, to Assoc. Prof. Dr. Vladimír Velebný from CPN Company, Dolní Dobrouč, Czech Republic for providing of hyaluronan and Andrew Cuthbert (MPhys) from Wageningen University, The Netherlands for correction of English style and grammar.

References

Almond, A., DeAngelis, P. L., & Blundell, C. D. (2006). Hyaluronan: the local solution conformation determined by NMR and computer modeling is close to a contracted left-handed 4-fold helix. *Journal of Molecular Biology*, *358*(5), 1256–1269.

Bakhmutov, V. I. (2004). *Practical NMR relaxation for chemists*. Chichester, West Sussex, England: Wiley.

Belton, P. S. (1997). NMR and the mobility of water in polysaccharide gels. *International Journal of Biological Macromolecules*, *21*(1/2), 81–88.

Bouwstra, J. A., Salomonsdevries, M. A., & Vanmiltenburg, J. C. (1995). The thermal behaviour of water in hydrogels. *Thermochimica Acta*, *248*, 319–327.

Chakraborty, S., Sinha, S. K., & Bandyopadhyay, S. (2007). Low-frequency vibrational spectrum of water in the hydration layer of a protein: A molecular dynamics simulation study. *Journal of Physical Chemistry B*, *111*(48), 13626–13631.

Dave, Y., Tamagno, M., Marsano, E., & Focher, B. (1995). Hyaluronan acide (hydroxypropyl) cellulose blends – A solution and solid-state study. *Abstracts of Papers of the American Chemical Society*, *209*, 149–150.

Davies, A., Gormally, J., Wynjones, E., Wedlock, D. J., & Phillips, G. O. (1983). A study of factors influencing hydration of sodium hyaluronate from compressibility and high-precision densitometric measurements. *Biochemical Journal*, *213*(2), 363–369.

Froix, M. F., & Nelson, R. (1975). Interaction of water with cellulose from nuclear magnetic resonance relaxation times. *Macromolecules*, *8*(6), 726–730.

Garg, H. G., & Hales, C. A. (2004). *Chemistry and Biology of Hyaluronan*. Amsterdam, Nederland: Elsevier.

Hatakeyama, T., Hatakeyama, H. (2004). Thermal Properties of Green Polymers and Biocomposites.

Hunger, J., Bernecker, A., Bakker, H. J., Bonn, M., & Richter, R. P. (2012). Hydration dynamics of hyaluronan and dextran. *Biophysical Journal*, *103*(1), L10–L12.

Kucerik, J., Prusova, A., Rotaru, A., Flimel, K., Janecek, J., & Conte, P. (2011). DSC study on hyaluronan drying and hydration. *Thermochimica Acta*, *523*(1/2), 245–249.

Liu, J., & Cowman, M. K. (2000). Thermal analysis of semi-dilute hyaluronan solutions. *Journal of Thermal Analysis and Calorimetry*, *59*(1/2), 547–557.

Mariette, F. (2009). Investigations of food colloids by NMR and MRI. *Current Opinion in Colloid & Interface Science*, *14*(3), 203–211.

McBrierty, V. J., Martin, S. J., & Karasz, F. E. (1999). Understanding hydrated polymers: The perspective of NMR. *Journal of Molecular Liquids*, *80*(2/3), 179–205.

Mlcoch, T., & Kucerik, J. (2013). Hydration and drying of various polysaccharides studied using DSC. *Journal of Thermal Analysis and Calorimetry*, http://dx.doi.org/10.1007/s10973-013-2946-1

Nestor, G., Kenne, L., & Sandstrom, C. (2010). Experimental evidence of chemical exchange over the beta($1 \rightarrow 3$) glycosidic linkage and hydrogen bonding involving hydroxy protons in hyaluronan oligosaccharides by NMR spectroscopy. *Organic & Biomolecular Chemistry*, *8*(12), 2795–2802.

Okada, R., Matsukawa, S., & Watanabe, T. (2002). Hydration structure and dynamics in pullulan aqueous solution based on H-1 NMR relaxation time. *Journal of Molecular Structure*, *602*, 473–483.

Prusova, A., Smejkalova, D., Chytil, M., Velebny, V., & Kucerik, J. (2010). An alternative DSC approach to study hydration of hyaluronan. *Carbohydrate Polymers*, *82*(2), 498–503.

Scott, J. E., & Heatley, F. (1999). Hyaluronan forms specific stable tertiary structures in aqueous solution: A C-13 NMR study. *Proceedings of the National Academy of Sciences of the United States of America*, *96*(9), 4850–4855.

Scott, J. E., & Heatley, F. (2002). Biological properties of hyaluronan in aqueous solution are controlled and sequestered by reversible tertiary structures, defined by NMR spectroscopy. *Biomacromolecules*, *3*(3), 547–553.

Shapiro, Y. E. (2011). Structure and dynamics of hydrogels and organogels: An NMR spectroscopy approach. *Progress in Polymer Science*, *36*(9), 1184–1253.

Sutherland, I. W. (1998). Novel and established applications of microbial polysaccharides. *Trends in Biotechnology*, *16*(1), 41–46.

Takahashi, M., Hatakeyama, T., & Hatakeyama, H. (2000). Phenomenological theory describing the behaviour of non-freezing water in structure formation process of polysaccharide aqueous solutions. *Carbohydrate Polymers*, *41*(1), 91–95.

Topgaard, D., & Soderman, O. (2002). Changes of cellulose fiber wall structure during drying investigated using NMR self-diffusion and relaxation experiments. *Cellulose*, *9*(2), 139–147.

Wunderlich, B. (2005). *Thermal analysis of Polymeric Materials*. Berlin: Springer-Verlag.

Yokomizo, T., Nakasako, M., Yamazaki, T., Shindo, H., & Higo, J. (2005). Hydrogen-bond patterns in the hydration structure of a protein. *Chemical Physics Letters*, *401*(4–6), 332–336.